Organic & Biomolecular Chemistry

COMMUNICATION

View Article Online
View Journal | View Issue

Cite this: *Org. Biomol. Chem.*, 2015, **13**, 9564

Received 17th July 2015,
Accepted 13th August 2015

DOI: 10.1039/c5ob01463h

www.rsc.org/obc

Dicyanovinyl-substituted J147 analogue inhibits oligomerization and fibrillation of β-amyloid peptides and protects neuronal cells from β-amyloid-induced cytotoxicity†

Kyoungdo Kim,‡[a] Kwang-su Park,‡[a] Mi Kyoung Kim,[a] Hyunah Choo[b,c] and Youhoon Chong*[a]

A series of novel J147 derivatives were synthesized, and their inhibitory activities against β-amyloid (Aβ) aggregation and toxicity were evaluated by using the oligomer-specific antibody assay, the thioflavin-T fluorescence assay, and a cell viability assay in the transformed SH-SY5Y cell culture. Among the synthesized J147 derivatives, 3j with a 2,2-dicyanovinyl substituent showed the most potent inhibitory activity against $A\beta_{42}$ oligomerization (IC_{50} = 17.3 μM) and $A\beta_{42}$ fibrillization (IC_{50} = 10.5 μM), and disassembled the preformed $A\beta_{42}$ fibrils with an EC_{50} of 10.2 μM. Finally, we confirmed that 3j is also effective at preventing neurotoxicity induced by $A\beta_{42}$-oligomers as well as $A\beta_{42}$-fibrils.

Alzheimer's disease (AD) is a chronic neurodegenerative disease characterized by synaptic and neuronal loss, which results in dementia, cognitive dysfunction, language problems, and memory loss.[1] These symptoms of AD generally appear in people who are aged 65 and above, and the number of AD patients is continually increasing.[2] At present, acetylcholinesterase inhibitors are used to provide temporary relief of symptoms, but there is no effective, long-term treatment for AD.[3] Pathologically, AD is characterized by the accumulation of extracellular senile plaques containing β-amyloid peptides (Aβ) and intracellular neurofibrillary tangles (NFTs) resulting from tau fibrillogenesis.[4] The Aβ peptide, the molecular culprit in AD, derives from the amyloid precursor protein (APP) through sequential cleavage by the two proteases β- and γ-secretase.[5] The Aβ monomers then start aggregating to eventually become pathogenic oligomers[6] and insoluble fibrillar aggregates.[7] Thus, blocking the aggregation of the Aβ peptide is a potential disease-modifying approach to the treatment of AD.[8–15]

Curcumin (Fig. 1), the yellow pigment and primary curcuminoid found in turmeric, is well known for its potent antioxidant and anti-inflammatory activities. It has also been reported that curcumin inhibits the formation of Aβ oligomers and fibrils *in vivo*,[16] and there have been several attempts to apply curcumin to the treatment of AD.[17] However, due to poor bioavailability and low neurotrophic activity, the therapeutic use of curcumin for AD treatment has not been very successful.[18] Efforts have been made to optimize the potency and pharmacokinetic properties of curcumin, which culminated in the recent identification of J147 (Fig. 1) as an exceptionally potent neurotrophic molecule that facilitates memory in normal rodents, and prevents the loss of synaptic proteins and cognitive decline in transgenic AD mouse models.[19,20] However, the potent therapeutic effects of J147 against AD do not seem to be directly associated with its anti-amyloidogenic effects; even though J147 reduced soluble levels of Aβ, it was attributed to down-regulation of β-secretase (BACE) rather than inhibition of Aβ aggregation.[19,20] Thus, in terms of an anti-amyloidogenic effect, J147 has suboptimal properties, and in the course of our ongoing efforts to discover new and more effective inhibitors of Aβ aggregation, we anticipated that structural modification of the J147 scaffolding might provide a novel Aβ-aggregation inhibitor with potent anti-AD activity. For this purpose, the J147 scaffold was compared with two high affinity Aβ-binders, curcumin and DDNP (1,1-dicyano-2-[6-(dimethylamino)naphthalene-2-yl]propene),[21] which led to the conclusion that appropriate substitution at the aromatic *para*-position of the J147 scaffold might enhance its Aβ-binding affinity and thereby the anti-amyloidogenic activity (Fig. 1).

[a]*Department of Bioscience and Biotechnology, Bio/Molecular Informatics Center, Konkuk University, Hwayang-dong, Gwangjin-gu, Seoul 143-701, Korea. E-mail: chongy@konkuk.ac.kr*
[b]*Center for Neuro-Medicine, Korea Institute of Science and Technology, 39-1 Hawolgok-dong, Seoungbuk-gu, Seoul 136-791, Korea*
[c]*Department of Biological Chemistry, Korea University of Science and Technology, Youseong-gu, Daejeon 305-350, Korea*

†Electronic supplementary information (ESI) available: Synthetic procedures and characterization of new compounds. Experimental details for $A\beta_{42}$ oligomerization, $A\beta_{42}$ fibrillation, atomic force microscopy (AFM), ELISA assay for inhibition of $A\beta_{42}$ oligomerization, thioflavin T fluorescence assay for inhibition of $A\beta_{42}$ fibrillation, disruption assay of $A\beta_{42}$ fibrils and $A\beta_{42}$-induced cytotoxicity assay. See DOI: 10.1039/c5ob01463h

‡These authors contributed equally on this work.

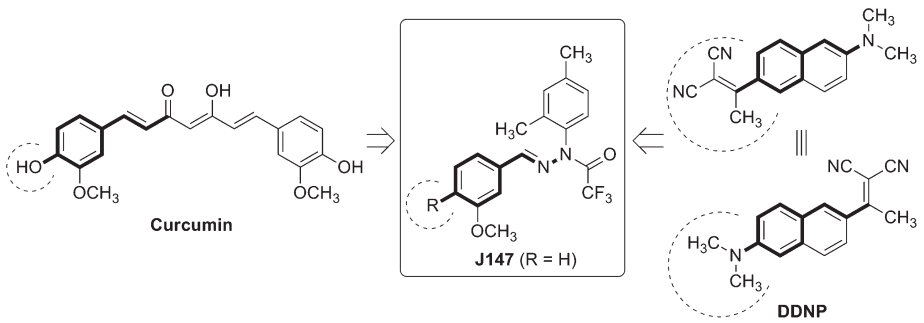

Fig. 1 Structures of curcumin, DDNP and J147. Bold lines and dotted circles denote structural similarities and aromatic *para*-substituents, respectively.

In this context, functional groups which mimic the aromatic *para*-substituent of curcumin or DDNP (OH, OCH_3, CH_3, F, $CH(CN)_2$ and NMe_2) were of particular interest.

In this proof-of-concept study, we embarked on a structural modification study on the J147's aromatic ring by introducing various substituents at its *para*-position. Herein, we report the synthesis of novel J147 derivatives and evaluation of their inhibitory activity against Aβ aggregation and Aβ-induced neurotoxicity by using the oligomer-specific antibody assay, the thioflavin-T (ThT) fluorescence assay and a cell viability assay in the transformed SH-SY5Y cell culture.

Results and discussion

The J147 derivatives (**3**) were prepared by condensation of the variously substituted 3-methoxybenzaldehydes (**1**) with the commercially available (2,4-dimethylphenyl) hydrazine hydrochloride (**2**) followed by amidation with trifluoroacetic anhydride (Scheme 1).[19] Among the nine 3-methoxybenzaldehydes used for the condensation reaction, only three (**1a**, **1c**, **1g**) were commercially available; thus, the others were prepared from other commercial sources. First, synthesis of 3-methoxy-4-nitrobenzaldehyde (**1b**) was accomplished by aromatic nitration of 3-methoxybenzaldehyde (**1a**). On the other hand, 4-([*tert*-butyldimethylsilyl] oxy)-3-methoxybenzaldehyde (**1d**), 3,4-dimethoxybenzaldehyde (**1e**) and 2-methoxy-[1,1′-biphenyl]-4-carbaldehyde (**1f**) were prepared from vanillin (**1c**) *via* silyl protection, methylation, and Suzuki coupling, respectively. Methyl 3-methoxy-4-methylbenzoate (**1g**) and 4-fluoro-3-methoxybenzaldehyde (**1i**) were converted into the corresponding benzaldehydes (**1h** and **1j**) by reduction followed by oxidation and nucleophilic aromatic substitution, respectively. Finally, synthesis of 2-(4-formyl-2-methoxybenzylidene)-malononitrile (**1l**) required complex synthetic steps. Thus, starting from 4-bromo-3-methoxyaniline (**1k**), the amino functionality was transformed into the formyl group by a series of reactions including diazotization of aniline, replacement of the diazonium cation with cyanide, and reduction of the resulting aromatic cyanide to the corresponding aldehyde, while the 4-bromo group was subjected to the formyl transfer

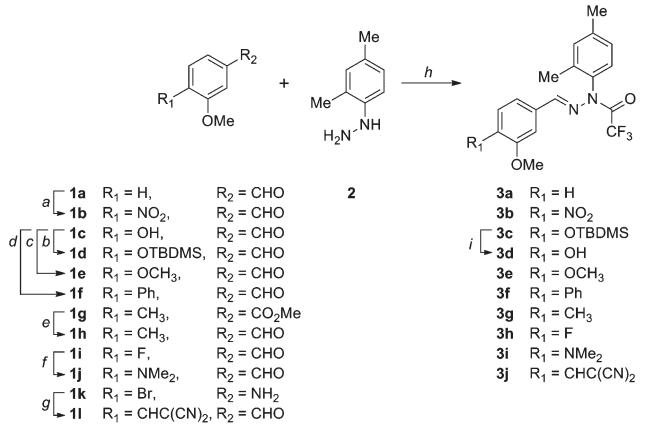

Scheme 1 Synthesis of the J147 derivatives. Reagents and conditions: (a) HNO_3, H_2SO_4, rt; (b) TBDMSCl, Im, CH_2Cl_2, rt; (c) CH_3I, K_2CO_3, acetone, rt; (d) (i) Tf_2O, TEA, CH_2Cl_2, 0 °C; (ii) $PhB(OH)_2$, $Pd(PPh_3)_4$, K_2CO_3, MeOH, rt; (e) (i) DIBAL-H, THF, −78 °C; (ii) PCC, CH_2Cl_2, 0 °C; (f) $NHMe_2$, K_2CO_3, DMSO−H_2O (7 : 3), 110 °C; (g) (i) HCl, $NaNO_2$, H_2O, 0 °C; CuCN, KCN, H_2O, 70 °C; (ii) DIBAL-H, tol. −78 °C; (iii) $HO(CH_2)_2OH$), *p*-TsOH, tol. reflux; (iv) *n*BuLi, THF, −78 °C; *N*-formylpiperidine; (v) malononitrile, Im, THF, rt; (vi) 2 N HCl, acetone, rt; (h) EtOH, rt; Tf_2O, TEA (or pyr), CH_2Cl_2, 0 °C; (i) TBAF, THF, 0 °C.

reaction with *N*-formylpiperidine followed by Knoevenagel condensation with malononitrile. The 3-methoxybenzaldehydes (**1a–1b**, **1d–1f**, **1h–1j**, and **1l**), thus prepared, were condensed with (2,4-dimethylphenyl)-hydrazine hydrochloride (**2**) to yield the unstable benzylidenehydrazines, which were directly reacted with trifluoroacetic anhydride to obtain the desired trifluorohydrazides (**3a–3c**, **3e–3j**) in 45–50% yields. Cleavage of silyl ether in **3c** by treatment with TBAF (tetrabutylammonium fluoride) proceeded smoothly to give **3d** in 64% yield.

The prepared J147 derivatives were evaluated for their activity to inhibit Aβ aggregation and to protect neuronal cells from Aβ-induced cytotoxicity. For this purpose, the 42-residue $Aβ_{42}$ stock solutions (2 mM) were prepared by dissolving the lyophilized peptide in 100 mM NaOH.[22] For oligomerization, the $Aβ_{42}$ stock solution was diluted in phosphate-buffered saline (PBS), pH 7.4 (100 μM final $Aβ_{42}$ concentration) and

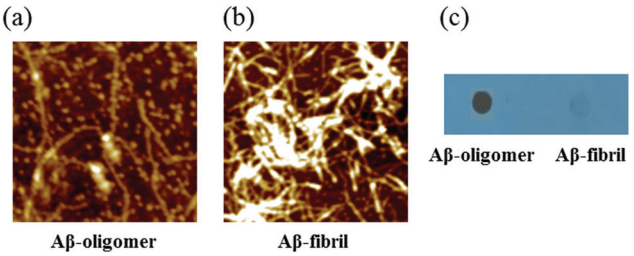

Fig. 2 $A\beta_{42}$ assembly under conditions that facilitate either oligomerization (a) or fibrillation (b). AFM images show formation of globular oligomers (a) and fibrils (b) of $A\beta_{42}$. Oligomers were analyzed by dot blot analysis with A11 antibody (c, left) but fibrils were not detectable (c, right).

incubated at 25 °C for four days.[22] On the other hand, fibrillization was initiated by diluting the stock solution in 10 mM HEPES, 100 mM NaCl, 0.02% sodium azide, pH 7.4 (50 μM final $A\beta_{42}$ concentration), which was incubated at 37 °C without agitation for up to two days.[22] The formations of globular $A\beta_{42}$ oligomers (Fig. 2a) and fibrillar $A\beta_{42}$ (Fig. 2b) were confirmed by AFM (atomic force microscopy). Oligomeric and fibrillar $A\beta_{42}$ were further confirmed by dot blot analysis using a polyclonal antibody A11 that specifically recognizes soluble, prefibrillar Aβ oligomers but not monomer, dimer, trimer, tetramer or Aβ fibrils (Fig. 2c).[22,23]

First, in order to examine the ability of the J147 derivatives to inhibit $A\beta_{42}$ oligomerization, an ELISA assay using the A11 antibody[22] was performed. Thus, the oligomerization reaction was conducted[22] in the absence (control samples treated with 1% dimethyl sulfoxide [DMSO]) or presence of the J147 derivatives (100 μM). Absorbance (OD) of each sample was recorded at 450 nm in triplicate and the average absorbance of samples treated with the J147 derivatives relative to that of the control is shown in Fig. 3a. Among the J147 derivatives, **3j** with a 2,2-dicyanovinyl substituent showed the most potent inhibitory activity against $A\beta_{42}$ oligomer formation, while others including **3a** (J147) had only marginal effects. Compared with the control, the amount of Aβ oligomers in the sample treated with **3j** decreased to 32% (Fig. 3a). The inhibitory potency of **3j** on $A\beta_{42}$ oligomerization was then assessed at concentrations ranging from 0.1 to 200 μM, and the IC_{50} value was determined from the dose–response curve (IC_{50} = 17.3 ± 1.3 μM, Fig. 3b). The $A\beta_{42}$ incubated in the presence of **3j** did not show globular oligomers in the AFM image (Fig. 3c).

The J147 derivatives were also evaluated for their activity to inhibit fibril formation, and to disassemble preformed $A\beta_{42}$ fibrils. The thioflavin T (ThT) fluorescence assay has been widely used to detect the formation of amyloid fibrils, because the binding of thioflavin dyes to amyloid fibrils enables reduction of self-quenching by restricting the rotation of the benzothiozole and benzaminic rings, leading to significant increase in fluorescence quantum yield.[24] Thus, $A\beta_{42}$ solution (50 μM), in the presence of 1% DMSO (control reaction) or the J147 derivatives (**3a**, **3b**, **3d–3i**) (100 μM), was incubated at 37 °C for 24 h under fibrillation conditions[22] (Fig. 4a). Strong ThT emission was observed in the control reaction, but the samples treated with **3e**, **3i**, and **3j** showed a decreased fluorescence signal (Fig. 4a). In particular, **3j**, which showed the most potent inhibitory activity against $A\beta_{42}$ oligomerization, was also the most effective fibrillation inhibitor evaluated.

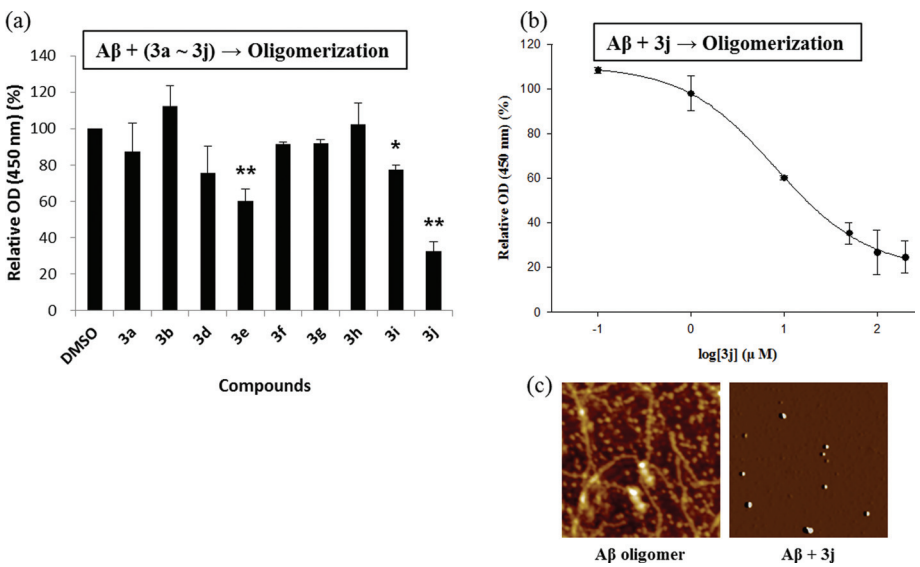

Fig. 3 ELISA assay for inhibition of $A\beta_{42}$ oligomerization by the J147 derivatives. (a) Amounts of the $A\beta_{42}$ oligomers in the samples treated with 1% DMSO (control) or the J147 derivatives (**3a**, **3b**, **3d–3i**) (100 μM) were determined by ELISA using the oligomer-specific A11 antibody. Vertical bars represent optical density (OD) values ± SD relative to the control. *P < 0.05, **P < 0.001 relative to the control. (b) Concentration-dependent inhibition of $A\beta_{42}$ oligomerization by **3j**. Y-Axis represent relative OD values ± SD obtained from $A\beta_{42}$ oligomers (50 μM) treated with **3j**. All measurements were performed in triplicate. (c) AFM images of the control (left) and a sample treated with **3j** (100 μM).

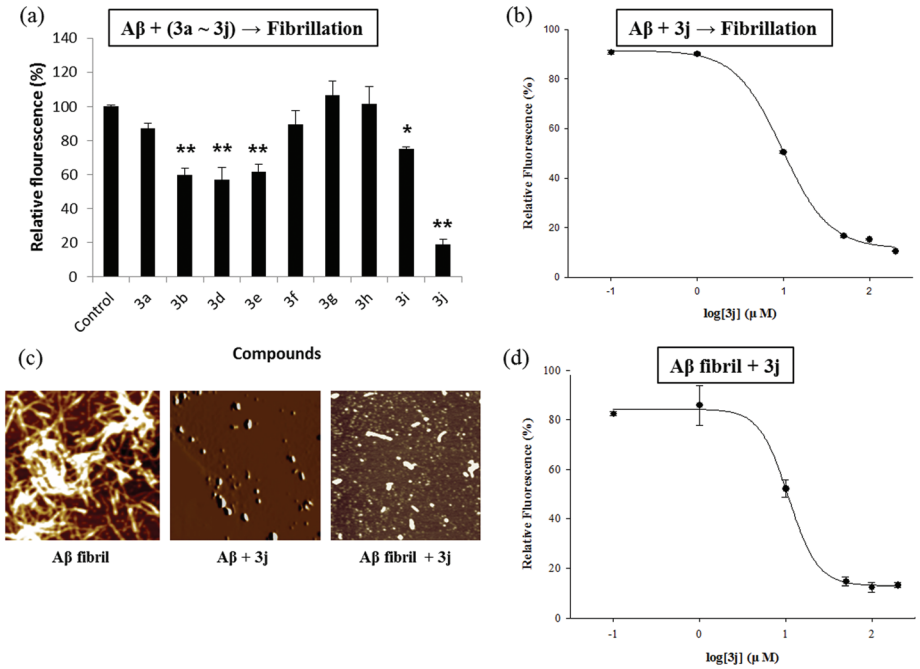

Fig. 4 (a–c) ThT assay for assessing inhibition of $A\beta_{42}$ fibrillogenesis by the J147 derivatives: (a) amounts of the $A\beta_{42}$ fibrils in the samples treated with 1% DMSO (control) or the J147 derivatives (**3a**, **3b**, **3d–3i**) (100 μM) were determined by fluorescence from ThT. Vertical bars represent fluorescence intensities ± SD relative to the control. *P < 0.05, **P < 0.001 relative to the control. (b) Fluorescence was measured from $A\beta_{42}$ peptides under fibrillization conditions in the presence of different concentrations (0.1–200 μM) of **3j**. The Y-axis represents the fluorescence intensity ± SD relative to the control (DMSO). All measurements were performed in triplicate. (c) AFM images of the $A\beta_{42}$ peptides under fibrillization conditions in the absence (control, left) or presence of **3j** (100 μM) (middle), and preformed $A\beta_{42}$ fibrils after treatment with **3j** (50 μM) (right). (d) ThT assay for disaggregation of preformed $A\beta_{42}$ fibrils by **3j**. Fluorescence was measured from the preformed $A\beta_{42}$ fibrils in the presence of different concentrations (0.1–200 μM) of **3j**. The y-axis represents fluorescence intensity ± SD relative to the control (DMSO). All measurements were performed in triplicate. *P < 0.05, **P < 0.001 relative to the control.

Fig. 4b shows dose-dependent inhibition of **3j** against $A\beta_{42}$ fibrillation and, from the dose–response curve, the IC_{50} of **3j** for inhibition of fibril formation was determined (10.5 μM). Inhibition of fibrillation by **3j** was further confirmed by the AFM images, and fibrils could not be seen after treatment with **3j** (100 μM) (Fig. 4c, middle). On the other hand, the J147 derivative **3j** was also effective in disassembling preformed $A\beta_{42}$ fibrils, and the ThT fluorescence assay showed a concentration-dependent decrease in the fluorescence signal with an EC_{50} of 10.2 μM (Fig. 4d). The AFM image of the disintegrated sample shows no fibrils but smaller spherical particles (Fig. 4c, right), presumed oligomers.[25]

Taken together, the dicyanovinyl functionality, a mimic of the aromatic substituent of DDNP, seems to enhance the binding affinity of the J147 scaffold to $A\beta_{42}$ to provide the J147 derivative **3j** with potent anti-amyloidogenic activity.

Soluble oligomers have been implicated as the primary toxic species of amyloids.[26–30] We examined whether the aggregation inhibitor **3j** could inhibit $A\beta_{42}$-induced neurotoxicity in cell culture. Toxicity was assessed with a 3-(4,5-dimethylthiazol-2-yl)-2,5-diphenyltetrazolium bromide (MTT) assay in transformed human neuroblastoma SH-SY5Y cells.[31] The J147 derivative **3j** was not cytotoxic up to 100 μM (Fig. S1 in the ESI†), but incubation of SH-SY5Y cells with 50 μM of $A\beta_{42}$ oligomers for 24 h led to significant toxicity (41 ± 2% cell viability) (Fig. 5a). When the $A\beta_{42}$ oligomer-treated cells were co-incubated with an increasing concentration of **3j**, the cell viability was recovered in a dose-dependent manner (Fig. 5a). Thus, upon treatment with 50 and 100 μM of **3j**, cell viability increased to 58 ± 3% and 77 ± 3%, respectively. The neuroprotective effects of **3j** against the cytotoxicity induced by $A\beta_{42}$ fibrils was also investigated (Fig. 5b). As reported previously, $A\beta_{42}$ fibrils were less cytotoxic (70 ± 2% cell viability) than the oligomers, and **3j** was effective at preventing $A\beta_{42}$ fibril-induced cytotoxicity in a dose-dependent manner (Fig. 5b). Next, we investigated the time course of neuroprotection induced by **3j**. Thus, after treatment of SH-SY5Y cells with preformed $A\beta_{42}$ fibrils and **3j** (10 μM), the cell viability was estimated by an MTT assay at various time points (Fig. 5c). Interestingly, a biphasic change was observed, and the SH-SY5Y cells exhibited an initial rapid decrease followed by an increase in viability between 7 and 48 hours. The initial decrease in viability of the cells treated with $A\beta_{42}$ fibrils is well matched with the $A\beta_{42}$ fibril-disaggregating activity of **3j** (Fig. 4d) to give the neurotoxic $A\beta_{42}$ oligomers (Fig. 4c, right panel). On the other hand, the ensuing increase in cell viability supports further disintegration of $A\beta_{42}$ oligomers to smaller nontoxic pieces.

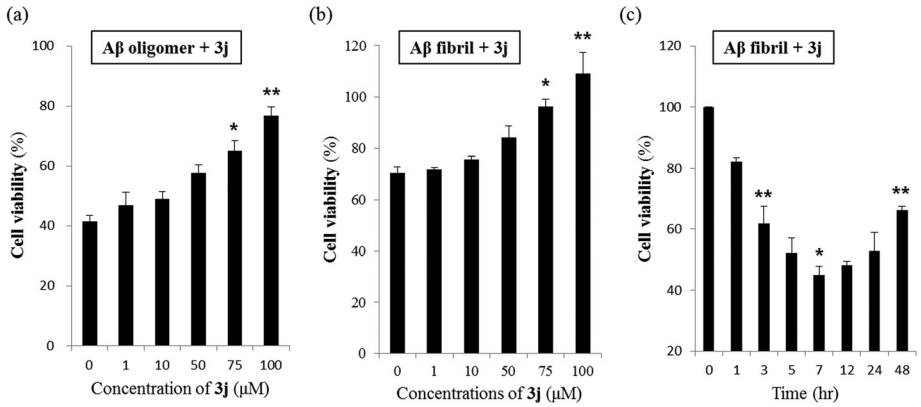

Fig. 5 Dose-dependent effects of **3j** on prevention of (a) $A\beta_{42}$ oligomer-induced and (b) $A\beta_{42}$ fibril-induced cytotoxicity. (c) Time-dependent effect of **3j** on $A\beta_{42}$ fibril-induced cytotoxicity. Vertical bars represent cell viability ± SD (%) relative to the control (untreated cells). All measurements were performed in triplicate. *P < 0.05, **P < 0.001 relative to the control.

Conclusions

J147 has strong potential to be an anti-AD therapeutic by slowing disease progression and reversing memory deficits, but its therapeutic effect does not seem to be directly associated with an anti-amyloidogenic effect. In this study, in the course of our ongoing efforts to discover new and more effective inhibitors of Aβ aggregation, we have undertaken a structural modification study on a J147 scaffold. Thus, various J147 derivatives were synthesized by introducing a substituent at the *para* position of the J147's aromatic functionality and evaluated their activity to inhibit $A\beta_{42}$ oligomerization and fibrillization, to disassemble the preformed $A\beta_{42}$ fibrils, and to prevent $A\beta_{42}$-induced neurotoxicity. Among them, **3j** with a 2,2-dicyanovinyl substituent showed the most potent inhibitory activity against $A\beta_{42}$ oligomerization (IC_{50} = 17.3 μM). The J147 derivative **3j** was also effective in inhibiting $A\beta_{42}$ fibrillization (IC_{50} = 10.5 μM) as well as disassembling the preformed $A\beta_{42}$ fibrils (EC_{50} = 10.2 μM). The potent anti-amyloidogenic activity of **3j** might be attributed to its dicyanovinyl functionality to enhance the binding affinity of the J147 scaffold to $A\beta_{42}$. Finally, we confirmed that **3j** is also effective at preventing neurotoxicity induced by $A\beta_{42}$-oligomers as well as $A\beta_{42}$-fibrils.

Acknowledgements

This study was supported by a grant of the Korean Health Technology R&D project, Ministry of Health & Welfare, Republic of Korea (HI14C2341), and by a grant from the Priority Research Centers Program through the National Research Foundation of Korea (NRF) funded by the Ministry of Education, Science and Technology (2009-0093824).

Notes and references

1 L. Minati, T. Edginton, M. G. Bruzzone and G. Giaccone, *Am. J. Alzheimer's Dis. Other Dementias*, 2009, **24**, 95.
2 Alzheimer's Association, *Alzheimer's Dementia*, 2014, **10**, e47.
3 B. Lam, E. Hollingdrake, J. L. Kennedy, S. E. Black and M. Masellis, *Hum. Genomics*, 2009, **4**, 91.
4 P. T. Nelson, I. Alafuzoff, E. H. Bigio, C. Bouras, H. Braak, N. J. Cairns, R. J. Castellani, B. J. Crain, P. Davies, K. Del Tredici, C. Duyckaerts, M. P. Frosch, V. Haroutunian, P. R. Hof, C. M. Hulette, B. T. Hyman, T. Iwatsubo, K. A. Jellinger, G. A. Jicha, E. Kövari, W. A. Kukull, J. B. Leverenz, S. Love, I. R. Mackenzie, D. M. Mann, E. Masliah, A. C. McKee, T. J. Montine, J. C. Morris, J. A. Schneider, J. A. Sonnen, D. R. Thal, J. Q. Trojanowski, J. C. Troncoso, T. Wisniewski, R. L. Woltjer and T. G. Beach, *J. Neuropathol. Exp. Neurol.*, 2012, **71**, 362.
5 S. J. Gandy, *J. Clin. Invest.*, 2005, **115**, 1121.
6 R. Roychaudhuri, M. Yang, M. M. Hoshi and D. B. Teplow, *J. Biol. Chem.*, 2009, **284**, 4749.
7 J. Hardy and D. J. Selkoe, *Science*, 2002, **297**, 353.
8 M. W. Beck, S. B. Oh, R. A. Kerr, H. J. Lee, S. H. Kim, S. Kim, M. Jang, B. T. Ruotolo, J.-Y. Lee and M. H. Lim, *Chem. Sci.*, 2015, **6**, 1879.
9 H. H. Lee, T. S. Choi, S. J. C. Lee, J. W. Lee, J. Park, Y.-H. Ko, W. J. Kim, K. Kim and H. I. Kim, *Angew. Chem., Int. Ed.*, 2014, **53**, 7461.
10 S. Sinha, D. H. J. Lopez, Z. Du, E. S. Pang, A. Shanmugam, A. Lomakin, P. Talbiersky, A. Tennstaedt, K. McDaniel, R. Bakshi, P.-Y. Kuo, M. Ehrmann, G. B. Benedek, J. A. Loo, F.-G. Klärner, T. Schrader, C. Wang and G. Bitan, *J. Am. Chem. Soc.*, 2011, **133**, 16958.
11 J. Bieschke, J. Russ, R. P. Friedrich, D. E. Ehrnhoefer, H. Wobst, K. Neugebauer and E. E. Wanker, *Proc. Natl. Acad. Sci. U. S. A.*, 2010, **107**, 7710.
12 C. Soto, E. M. Sigurdsson, L. Morelli, R. A. Kumar, E. M. Castaño and B. Frangione, *Nat. Med.*, 1998, **4**, 822.
13 A. Kapurniotu, A. Buck, M. Weber, A. Schmauder, T. Hirsch, J. Bernhagen and M. Tatarek-Nossol, *Chem. Biol.*, 2003, **10**, 149.
14 K. C. Nadimpally, A. Paul and B. Mandal, *ACS Chem. Neurosci.*, 2014, **5**, 400.

15 A. Paul, K. C. Nadimpally, T. Mondal, K. Thalluri and B. Mandal, *Chem. Commun.*, 2015, **51**, 2245.
16 F. Yang, G. P. Lim, A. N. Begum, O. J. Ubeda, M. R. Simmons, S. S. Ambegaokar, P. P. Chen, R. Kayed, C. G. Glabe, S. A. Frautschy and G. M. Cole, *J. Biol. Chem.*, 2005, **280**, 5892.
17 C. Zhang, A. Browne, D. Child and R. E. Tanzi, *J. Biol. Chem.*, 2010, **285**, 28472.
18 P. Anand, A. B. Kunnumakkara, R. A. Newman and B. B. Aggarwal, *Mol. Pharmaceutics*, 2007, **4**, 807.
19 Q. Chen, M. Prior, R. Dargusch, A. Roberts, R. Riek, C. Eichmann, C. Chiruta, T. Akaishi, K. Abe, P. Maher and D. Schubert, *PLoS One*, 2011, **6**, e27865.
20 M. Prior, R. Dargusch, J. L. Ehren, C. Chiruta and D. Schubert, *Alzheimer's Res. Ther.*, 2013, **5**, 25.
21 K. Shoghi-Jadid, G. W. Small, E. D. Agdeppa, V. Kepe, L. M. Ercoli, P. Siddarth, S. Read, N. Satyamurthy, A. Petric, S. C. Huang and J. R. Barrio, *Am. J. Geriatr. Psychiatry*, 2002, **10**, 24.
22 M. Necula, R. Kayed, S. Milton and C. G. Glabe, *J. Biol. Chem.*, 2007, **282**, 10311.
23 R. Kayed, E. Head, J. L. Thompson, T. M. McIntire, S. C. Milton, C. W. Cotman and C. G. Glabe, *Science*, 2003, **300**, 486.
24 H. Noor, P. Cao and D. P. Raleigh, *Protein Sci.*, 2012, **21**, 373.
25 M. Hoshi, M. Sato, S. Matsumoto, A. Noguchi, K. Yasutake, N. Yoshida and K. Sato, *Proc. Natl. Acad. Sci. U. S. A.*, 2003, **100**, 6370.
26 M. P. Lambert, A. K. Barlow, B. A. Chromy, C. Edwards, R. Freed, M. Liosatos, T. E. Morgan, I. Rozovsky, B. Trommer, K. L. Viola, P. Wals, C. Zhang, C. E. Finch, G. A. Krafft and W. L. Klein, *Proc. Natl. Acad. Sci. U. S. A.*, 1998, **95**, 6448.
27 D. M. Hartley, D. M. Walsh, C. P. Ye, T. Diehl, S. Vasquez, P. M. Vassilev, D. B. Teplow and D. J. Selkoe, *J. Neurosci.*, 1999, **19**, 8876.
28 M. Bucciantini, E. Giannoni, F. Chiti, F. Baroni, L. Formigli, J. Zurdo, N. Taddei, G. Ramponi, C. M. Dobson and M. Stefani, *Nature*, 2002, **416**, 507.
29 H. A. Lashuel, D. Hartley, B. M. Petre, T. Walz and P. T. Lansbury Jr., *Nature*, 2002, **418**, 291.
30 R. Kayed, J. Bernhagen, N. Greenfield, K. Sweimeh, H. Brunner, W. Voelter and A. Kapurniotu, *J. Mol. Biol.*, 1999, **287**, 781.
31 M. Encinas, M. Iglesias, Y. Liu, H. Wang, A. Muhaisen, V. Cenã, C. Gallego and J. X. Comella, *J. Neurochem.*, 2000, **75**, 991.